

Centrality dependence of hadronization and chemical freeze-out conditions in heavy ion collisions at $\sqrt{s_{NN}} = 2.76$ TeV

Francesco Becattini,¹ Marcus Bleicher,² Eduardo Grossi,¹ Jan Steinheimer,² and Reinhard Stock^{2,3}

¹*Università di Firenze and INFN Sezione di Firenze, Firenze, Italy*

²*Frankfurt Institute for Advanced Studies (FIAS), Frankfurt, Germany*

³*Institut für Kernphysik, Goethe-Universität, Frankfurt, Germany*

(Received 19 May 2014; revised manuscript received 9 July 2014; published 14 November 2014)

We present an analysis of hadronic multiplicities measured in Pb-Pb collisions at $\sqrt{s_{NN}} = 2.76$ TeV as a function of the collision centrality within the statistical hadronization model. Evidence is found of a dependence of the chemical freeze-out temperature as a function of centrality, with a slow rise from central to peripheral collisions, which we interpret as an effect of posthadronization inelastic scatterings. Using correction factors calculated by means of a simulation based on the URQMD model, we are able to obtain a significant improvement in the statistical model fit quality and to reconstruct the primordial chemical equilibrium configuration. This is characterized by a nearly constant temperature of about 164 MeV, which we interpret as the actual hadronization temperature.

DOI: [10.1103/PhysRevC.90.054907](https://doi.org/10.1103/PhysRevC.90.054907)

PACS number(s): 25.75.Dw, 25.75.Nq

I. INTRODUCTION

The determination of the critical temperature of QCD is one of the principal goals of relativistic nucleus-nucleus (AA) collision physics. This temperature has been calculated in lattice QCD [1–3] to be about 160 MeV at a baryon-chemical potential $\mu_B \simeq 0$, a situation characteristic of heavy ion collisions at top energies available at the BNL Relativistic Heavy Ion Collider (RHIC) and the CERN Large Hadron Collider (LHC). At very low μ_B the phase transition from hadronic matter to quark-gluon plasma (QGP) has been found to be a continuous one (a *crossover*), so that the value of the (pseudo-) critical temperature depends somewhat on the specific observable under consideration [1,2].

It has been conjectured for quite some time [4] that the experimentally measured hadronic multiplicities, or multiplicity ratios, do, in fact, represent such an observable: They depend on the temperature prevailing at or near QCD hadronization. It has been proposed to use fluctuation of conserved charges to determine it [5,6], as these can be directly calculated in lattice QCD. However, multiplicities are first moments and, as such, are more robust observables against spurious effects. Indeed, a statistical *ansatz* is able to reproduce the measured hadronic yields, in both elementary [7] and relativistic nucleus-nucleus collisions [8]. This has led to the formulation of the statistical hadronization model (SHM) which, in a nutshell, assumes that hadrons are emitted from the fireball source at (almost) full chemical equilibrium. The reason for such a success, unexpected in elementary collisions, as well as the identity of the fitted temperature in all kinds of collisions, has been debated for a long time (see Refs. [9,10] for a summary). In practice, one can take advantage of this phenomenon to obtain the position of the parton-hadron coexistence line of QCD matter in the (T, μ_B) plane.

The temperature determined by fitting the hadronic multiplicities with the SHM is actually the one at which hadrons and resonances cease inelastic interaction, the so-called “chemical freeze-out” temperature. In principle, this may differ from the

QCD transition temperature if hadrons, after their formation, keep interacting inelastically. This is, clearly, not the case in elementary e^+e^- annihilation to hadrons but it could become relevant in the high-multiplicity final state of AA collisions. Different reactions could then freeze-out at different times, in inverse order of inelastic cross section, so that this stage of the fireball source expansion, dubbed as “afterburning,” would generally imply deviations from full chemical equilibrium of the hadronic species [11]. In the standard SHM analysis such effects were assumed to be negligibly small and that, therefore, the temperature and baryon-chemical potential yielded an ideal snapshot of the fireball dynamical trajectory at or near QCD hadronization.

An unexpected recent outcome from LHC has been the relatively low p/π ratio measured by the ALICE experiment in central Pb + Pb collisions [12,13] at $\sqrt{s_{NN}} = 2.76$ TeV, with respect to the expectation from the SHM [14]. A similar result was obtained earlier by the CERN Super Proton Synchrotron (SPS) experiment NA49 [15], which reported sizably low \bar{p} and $\bar{\Lambda}$ yields compared to SHM predictions [16]. This has been interpreted [17–20] as evidence of posthadronization baryon-antibaryon annihilation. An alternative explanation has been put forward in Ref. [21]. Note that annihilation cross sections do not fade away with dropping temperature, unlike inelastic transmutations. In Ref. [22] we proposed a picture of hadron production in relativistic $A + A$ collisions based on the idea of the hadronization process leading to chemical equilibrium of its outcome, followed by a stage of afterburning driving some hadronic species (notably baryons and antibaryons) out of chemical equilibrium before freeze-out. We determined these effects by employing the hybrid version of the microscopic transport model URQMD [23], obtaining *modification factors* owing to afterburning which were then employed in the subsequent data analysis. We thus reconstructed the primordial chemical equilibrium, up to a point where multihadron collisions could become important, and showed, for central collisions at various energies, a resulting rise of the deduced temperatures and significantly

improved SHM fit quality. This bears out the idea of a primordial chemical equilibrium as an intrinsic feature of hadronization.

In the present paper we extend our analysis, changing the topic from central collisions at various energies, to consideration of the centrality dependence of hadron multiplicities at fixed energy. Whereas, in central collisions, the final hadronic expansion stage causes substantial antibaryon and (at higher energies) baryon annihilation and regeneration, these effects should diminish toward more peripheral collisions because of the reduced overall multiplicity (see discussion in Sec. II). Thus, if our hypothesis is correct that the QCD hadronization process generates an equilibrium hadron-resonance yield distribution, at some constant temperature T , the afterburning effects should lead to a larger modification in central than in peripheral collisions. As baryon attenuation leads to lower apparent freeze-out temperatures derived from the standard SHM analysis, we would expect this temperature to rise, mildly, from central toward peripheral collisions.

These expectations have been borne out by a detailed hydrodynamical investigation [24] of the final stages of AA collisions. Interestingly, it was pointed out in Ref. [24] that, if afterburning played some role, the chemical freeze-out temperature T_{chem} fitted within the SHM should exhibit a nontrivial behavior, with a rise from central to peripheral collisions. Indeed, this effect is clearly observed for the *kinetic* freeze-out temperature, the temperature at which hadrons cease their elastic interactions. However, at the highest energy available at RHIC, no significant dependence of T_{chem} on centrality was seen [24–27], indicating that chemical composition is much less affected than spectra by the afterburning stage. In fact, the STAR experiment has found a dependence of T_{chem} on centrality at lower energy [28], but the slope of the function is reversed if the strangeness neutrality is enforced. It should also be kept in mind that at low energy the use of midrapidity densities may give rise to spurious effects such as an artificial enhancement of the strange particles, so that this observed dependence is difficult to interpret at this time.

Recently, the ALICE experiment at the LHC has provided [13,29] a set of high-precision measurements of hadronic species midrapidity multiplicities as a function of centrality in Pb + Pb collisions at $\sqrt{s_{NN}} = 2.76$ TeV. The improved accuracy and the increased total multiplicity with respect to RHIC energy should make it possible to highlight a dependence of T_{chem} on centrality. It is precisely the goal of this paper to test the centrality dependence of the chemical freeze-out temperature. This should settle the much-debated “proton anomalies” and provide further evidence for the constancy of the primordial hadronization temperature to be identified with the pseudocritical QCD temperature. To this end we first analyze the ALICE data with the standard SHM method. Then, by employing modification factors for all hadronic species, and all centralities, obtained from the hadronic transport model URQMD, we shall show that significant modification of the primordial abundances occurs in central collisions, in agreement with the findings in Refs. [17,22], reducing towards more peripheral collisions and mostly affecting the baryon-antibaryon species via annihilation and regeneration.

With the modification factors in place in a second SHM analysis we arrive at a uniform temperature of 164 ± 3 MeV.

II. THE FREEZE-OUT PROCESS

We can understand the effect of multiplicity on chemical freeze-out in relativistic heavy ion collisions with simple arguments. In an expanding system of interacting particles freeze-out occurs when the mean scattering time τ_{scatt} exceeds the mean collision time τ_{exp} ,

$$\tau_{\text{scatt}} = \frac{1}{n\sigma\langle v \rangle} > \tau_{\text{exp}} = \frac{1}{\partial u}, \quad (1)$$

u being the hydrodynamical velocity field and $\langle v \rangle$ is the mean velocity of particles. If the cross section σ is the inelastic one, the freeze-out is called *chemical*, whereas if it includes elastic processes, the freeze-out is called *kinetic*. Chemical freeze-out, of course, precedes the kinetic as the inelastic cross section is smaller than the total.

We can obtain a gross approximation of the expansion time with the ratio V/\dot{V} , where $V(t)$ is the volume of the fireball at the time t . For a fireball which is spherical in shape with a radius R , this is $R/3\dot{R}$, and if the radius increases at approximately the mean particle velocity $\langle v \rangle$, we have the condition

$$\frac{1}{n\sigma\langle v \rangle} > \frac{R}{3\langle v \rangle} \Rightarrow \frac{1}{n\sigma} > \frac{R}{3}. \quad (2)$$

For a given number of particles N within the volume, this inequality yields the radius at which freeze-out occurs as a function of N and of the average cross section,

$$R_{\text{fo}} = \sqrt{\frac{N\sigma}{4\pi}}, \quad (3)$$

and the density at which freeze-out occurs, which decreases with N according to

$$n_{\text{fo}} = \frac{N}{\frac{4\pi}{3}R_{\text{fo}}^3} = 3\sqrt{\frac{4\pi}{N}} \frac{1}{\sigma^{3/2}}. \quad (4)$$

Of course, it should be kept in mind that these estimates (3) and (4) are crude, but they tell us that the freeze-out radius for each particle approximately scales with the square root of the number of scattering centers with which a particle can interact and the related cross section. For a low-multiplicity hadronic system, it may happen that the above value exceeds the density of hadrons when they are formed, that is, at hadronization. This simply signals that hadrons decouple right after their formation without reinteracting, which happens in elementary collisions at the intrinsic hadronization density scale which is dictated by QCD. For relativistic heavy ion collisions, conversely, the multiplicity can grow to large numbers so that there could be enough time for hadronic reinteraction and freeze-out occurs later. For instance, for the typical value of $N = 1000$ in most central collisions and $\sigma = 30$ mb = 3 fm², one has $R_{\text{fo}} \simeq 15$ fm, which is in the right ballpark (for kinetic freeze-out) taking into account the drastic approximations made; the density at freeze-out turns out to be $n_{\text{fo}} \simeq 0.06$ fm⁻³, which is lower than the typical hadronization density of about 0.5 fm⁻³.

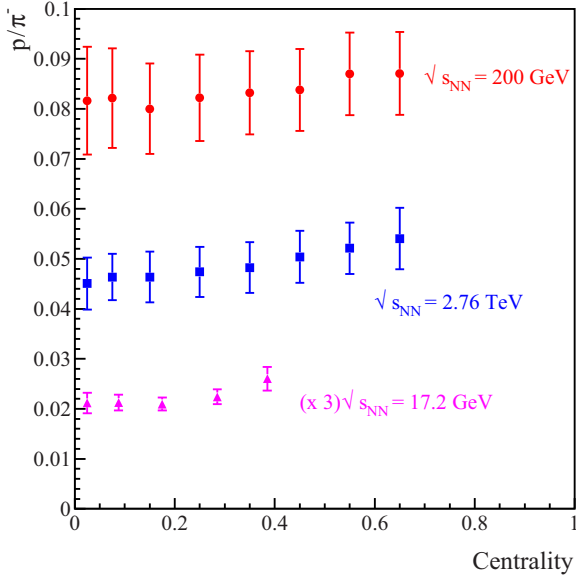


FIG. 1. (Color online) Ratio between antiproton and negative pion yields in relativistic heavy ion collisions as a function of centrality at different energies.

The above equations also imply that, if hadronization occurs at a universal temperature T_f [9,10], which is the pseudocritical QCD temperature, the effective average temperature of the chemical freeze-out should increase in peripheral collisions if equilibrium is approximately maintained in the hadronic reinteraction stage. The strength of this effect depends, according to Eq. (4), on the function $n_{f_0}(T)$ and it is, as expected, larger for the kinetic than chemical freeze-out simply because the total cross section is larger than the inelastic one. In general, because the hadronic density strongly depends on the temperature, the dependence of T_{chem} on N , hence on centrality, is mild. To highlight it, one needs a large lever arm in terms of multiplicity and higher energies are more favorable in this respect, as has been mentioned in the Introduction.

Before moving to the data analysis, it should be pointed out that there is evidence of afterburning in the data itself. In Fig. 1 we show the behavior of \bar{p}/π^- ratio as a function of centrality at different center-of-mass energies. In all three cases, the ratio slightly, yet significantly (taking into account that errors are visibly correlated), increases from central to peripheral collisions, in agreement with the expectation of a larger antibaryon annihilation in more central events. Note that, at the LHC energy, this effect cannot by any means be explained by a genuine decrease of baryon-chemical potential at freeze-out in

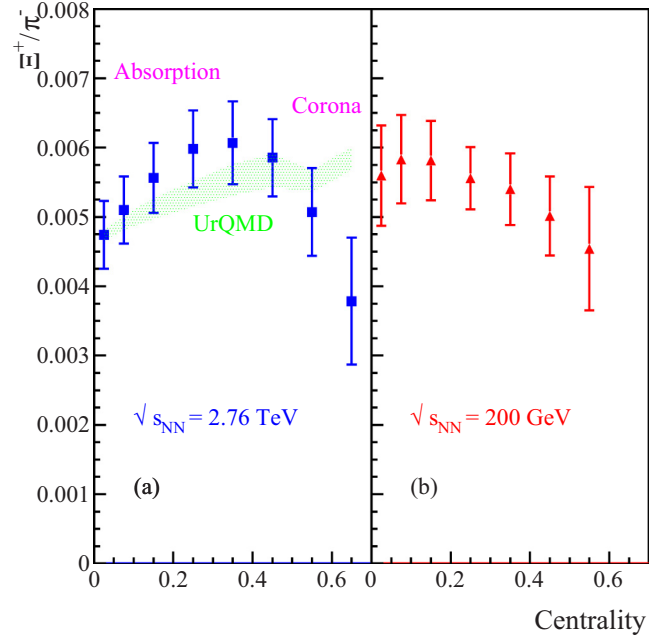


FIG. 2. (Color online) Ratio between Ξ^+ and negative pion yields in relativistic heavy ion collisions as a function of centrality at different energies. At the largest energy (a), a structure can be clearly seen. We interpret the bump in mid-peripheral events as the combination of two effects: increased baryon annihilation owing to larger multiplicity at LHC and the corona effect in very peripheral. Also shown is the prediction of coronaless URQMD calculations normalized to the most central bin.

peripheral collisions because all particle/antiparticle ratios are consistent with $\mu_B \simeq 0$ at all centralities. A possible mundane explanation to be considered is a core-corona superposition if the ratio \bar{p}/π^- was larger in pp than central AA at the same energy (see Table I). However, this is ruled out by the stunning centrality behavior of the ratio Ξ^+/π^- , shown in Fig. 2. Unlike at RHIC, this ratio surprisingly *increases* from central towards peripheral collisions, then drops according to the expectations of the core-corona model [35] as its value is indeed much lower in pp than in AA collisions (see Table I) at all energies.

The rise of the Ξ/π ratio is the result of the larger relative absorption of Ξ and the larger relative production of pions in the most central collisions. Altogether, the centrality dependence of these particle ratios confirm the expected dependence of chemical freeze-out on particle multiplicity.

TABLE I. Ratios \bar{p}/π^- and Ξ^+/π^- in pp and AA collisions at different energies. The ratio Ξ^+/π^- in pp is always less than in AA at the same $\sqrt{s_{NN}}$.

$\sqrt{s_{NN}}$ (GeV)	\bar{p}/π^- (AA)	\bar{p}/π^- (pp)	Ξ^+/π^- (AA)	Ξ^+/π^- (pp)
17.2	0.0067 ± 0.00062 [15,30]	0.0165 ± 0.0005 [31]	$(1.12 \pm 0.17) \times 10^{-3}$ [15,30]	$(3.9 \pm 0.4) \times 10^{-4}$ [31]
200	0.082 ± 0.012 [26,32]	0.080 ± 0.009 [32,33]	$(6.6 \pm 0.79) \times 10^{-3}$ [26,32]	$(2.0 \pm 0.7) \times 10^{-3}$ [32,33]
2750	0.045 ± 0.005 [13,29]	–	$(4.7 \pm 0.5) \times 10^{-3}$ [13,29]	–
7000	–	–	–	$(3.25 \pm 0.32) \times 10^{-3}$ [34]

III. DATA ANALYSIS

We have analyzed the multiplicities measured by the ALICE experiment at $\sqrt{s_{NN}} = 2.76$ TeV [13,29] to determine the chemical freeze-out parameters with fits to the usual SHM (described in Ref. [10]) predictions and to the same formulas corrected for the modification factors, defined as the ratios between the particle yields with afterburning and the same yields without it. The modification factors have been estimated with a hybrid version of the code URQMD [23], implementing afterburning after a hadron generation according to local thermodynamical equilibrium prescription (Cooper-Frye formula). Therefore, the estimated factors are the outcome of a full simulation of the heavy ion collision process

A. Data interpolation

The midrapidity densities of hyperons [13,29] are provided by the ALICE experiment with a centrality binning different from that of p , K , and π (ten centrality classes for the latter, seven for Λ 's, and five for Ω and Ξ 's). Thus, we have interpolated the yields of hyperons to obtain their values in the same centrality bins as for the protons, pions, and kaons. As interpolation function we chose a sixth-degree polynomial for Λ 's and a fourth-degree polynomial for Ω 's and Ξ 's. To make a proper comparison with the data, we calculated the integral mean value within each bin,

$$N([c_i, c_{i+1}]) = a_0 + a_1(c_{i+1}^2 - c_i^2)/2(c_{i+1} - c_i) + a_2(c_{i+1}^3 - c_i^3)/3(c_{i+1} - c_i) + \dots,$$

where c_i are the centrality limits of each bin. We have determined the coefficients a_i by making a χ^2 fit to the data in the various centrality bins. Because the experimental errors among different centrality bins are apparently correlated, we have formed a nondiagonal covariance matrix C in the χ^2 ,

$$\chi^2 = \sum_{\text{bins}} (\text{theo}_i - \text{meas}_i) C_{ij}^{-1} (\text{theo}_j - \text{meas}_j),$$

assuming a constant correlation coefficient $\rho = 0.5$. Once the parameters a_i of the interpolating function were obtained, we were able to estimate the yields of the hyperons along with their error in the same bins of protons, pions, and kaons (see Table II) up to the 70%–80% bin. Because the data from Ref. [13,29] show that the yields of particles and antiparticles

are compatible within errors, we have interpolated the sum $\Omega + \bar{\Omega}$ to reduce the statistical uncertainty in the interpolation.

B. Calculation of modification factors

To quantify the effects of the hadronic phase (afterburning) on the particle ratios we employ the Ultrarelativistic Quantum Molecular Dynamics (URQMD) model in its current version [23]. The hadronic transport part of the model is based on an effective solution of the relativistic Boltzmann equation,

$$p^\mu \partial_\mu f_i(x^\nu, p^\nu) = C_i, \quad (5)$$

which describes the time evolution of the distribution functions $f_i(x^\nu, p^\nu)$ for particle species i , including the full collision term on the right-hand side. The interactions of hadrons in the current version is limited to binary elastic and $2 \rightarrow n$ inelastic scatterings, including resonance creations and decays, string excitations, and particle-antiparticle annihilations. The cross sections and branching ratios for the corresponding interactions are taken from experimental measurements, where available, and detailed balance relations.

The modification factors, required for our analysis, are extracted by running the fluid dynamics mode of the URQMD hybrid model, as discussed in Ref. [18], for Pb + Pb collisions at $\sqrt{s_{NN}} = 2.76$ TeV and the centralities defined by the ALICE experiment.

We then analyze the particle multiplicities of stable hadrons either at the end of the fluid dynamical phase or after the hadronic rescattering phase of the nuclear collision. The transition point from the fluid dynamical phase to the hadronic transport part occurs in successive transverse slices, of thickness 0.2 fm, whenever all fluid cells of that slice fall below a critical energy density, that is, six times the nuclear ground-state density $\epsilon \approx 850 \text{ MeV/fm}^3$ (in accordance with measures particle yields [18]), which is then the maximal energy density at which particles are generated. For the hydrodynamical stage of the URQMD simulation, we have applied an equation of state that follows from combining a hadronic phase with an effective mean-field quark model; see Ref. [36]. In the URQMD hybrid model hadrons of species i are produced by sampling the particle distributions defined by the Cooper-Frye prescription on a predefined hypersurface σ_μ :

$$E \frac{dN}{d^3p} = g_i \int_\sigma f_i(x, p) p^\mu d\sigma_\mu. \quad (6)$$

TABLE II. Results of the interpolation for the midrapidity yields of Ω , Ξ , and Λ in the same centrality class of proton, kaon, and pion [13,29].

	Λ	Ξ^-	$\bar{\Xi}^+$	$\Omega + \bar{\Omega}$
0%–5%	26.1 ± 2.8	3.57 ± 0.27	3.47 ± 0.26	1.26 ± 0.22
5%–10%	22.0 ± 1.9	3.13 ± 0.21	3.08 ± 0.20	1.07 ± 0.17
10%–20%	17.1 ± 1.6	2.52 ± 0.15	2.52 ± 0.15	0.83 ± 0.12
20%–30%	12.0 ± 1.1	1.80 ± 0.12	1.83 ± 0.12	0.57 ± 0.09
30%–40%	8.0 ± 1.0	1.19 ± 0.09	1.22 ± 0.09	0.37 ± 0.07
40%–50%	4.9 ± 0.5	0.70 ± 0.05	0.72 ± 0.05	0.22 ± 0.04
50%–60%	2.7 ± 0.5	0.35 ± 0.04	0.36 ± 0.04	0.120 ± 0.031
60%–70%	1.32 ± 0.35	0.149 ± 0.034	0.140 ± 0.033	0.053 ± 0.025
70%–80%	0.68 ± 0.35	0.099 ± 0.034	0.100 ± 0.034	0.011 ± 0.025

TABLE III. Comparison between midrapidity densities calculated at the end of hydrodynamical stage and fitted midrapidity densities of particle species in most central Pb + Pb collisions at $\sqrt{s_{NN}} = 2.76$ TeV. The relative errors on calculated multiplicities are the same as the experimental measurements at the same centrality. The γ_S parameter has been fixed to 1. The overall normalization is arbitrary.

Temperature	μ_B	χ^2/dof
158.2 ± 2.2 MeV	0 (fixed)	2.52/8
Particle	Calculated	Fitted with SHM
π^+	528 ± 37	542.4
π^-	529 ± 37	542.4
K^+	100.0 ± 7.7	95.63
K^-	101.0 ± 7.7	95.63
p	33.7 ± 2.4	33.31
\bar{p}	30.9 ± 2.2	33.31
Λ	18.9 ± 1.6	18.45
Ξ^-	2.79 ± 0.19	2.744
Ξ^+	2.79 ± 0.19	2.744
$\Omega + \bar{\Omega}$	0.94 ± 0.15	0.9498

Serving as an input, the local temperature, the chemical potentials, and the flow velocity u_μ enter the particle distribution function f_i ; i.e., all the particles, at the end of the fluid dynamical phase, are produced according to local chemical equilibrium. We therefore obtain the particle yield N_i either at the latest chemical equilibrium point (LCEP; see Ref. [22]) N_i^{CE} or after the chemical and kinetic freeze-out N_i^{FO} . The modification factor F_i^s , of particle species i is then simply defined as $F_i^s = N_i^{\text{FO}}/N_i^{\text{CE}}$. Note that the modification factors have been determined by turning off weak decays but performing all strong decays, in accord with the yields quoted by the ALICE experiment. It should also be stressed that in this procedure the URQMD average midrapidity particle multiplicities, generated at the end of the hydrodynamical stage (after the Cooper-Frye procedure), do, indeed, exhibit a common temperature of 158.2 ± 2.2 MeV if we fit them with the statistical model, as shown in Table III. Therefore, our calculated modification factors are close to those which would result from a calculation at the actually determined latest chemical equilibrium temperature of about 164 MeV in the data analysis (see Sec. IV).¹

The modification factors for π^+ , proton, and Ξ^- are shown in Fig. 3 as a function of the collision centrality. Note that the modification factors get closer to 1 for peripheral collisions.

At this point it is important to discuss the importance of multiparticle (=N body with $N > 2$) reactions and their effect on the modification factors defined above. As has been pointed out in earlier studies [37], the $N\pi \rightarrow p + \bar{p}$ (with N being 4 or 5) reaction can be responsible for the

¹We note in passing that the average Cooper-Frye temperature in Ref. [18] was obtained by calculating an average of the temperatures in the various hydro cells weighted with pion yields and it is therefore not directly comparable with the temperature determined by fitting particle multiplicities.

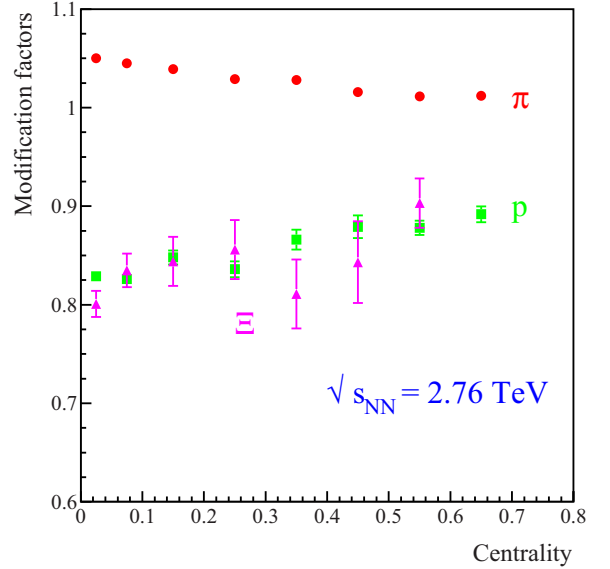


FIG. 3. (Color online) Modification factors (see text for definition) for π^+ , proton, and Ξ^- as a function of centrality at $\sqrt{s_{NN}} = 2.76$ TeV calculated with URQMD. The error bars are statistical.

regeneration of protons and antiprotons in the hadronic phase. Because the implementation of these multiparticle properties in a microscopic solution of the transport equation Eq. (5) is very difficult, we have to make a quantitative estimate on the importance of this back reaction. In Ref. [18] we estimated that the multipion fusion process, at the investigated beam energy, should only account for less than 10% regeneration of protons. This result agrees well with a recent study by Pan and Pratt [20], at the same beam energy and explicitly including detailed balance, which finds that even if a larger LCEP temperature of 170 MeV is chosen, only about 20% of all annihilated protons can be regenerated. Consequently, we can assume that neglecting the back reaction implies a small quantitative uncertainty in the modifications factors and does not basically alter our findings.

IV. RESULTS

The SHM, the relevant formulas for the calculation of midrapidity yields, and the fit procedure in relativistic heavy ion collisions at very high energy have been described in detail elsewhere [27]. Here we just note that at such a large energy, the rapidity distributions are wide enough to enable a determination of the thermodynamical parameters of the most central fireball, as was possible at $\sqrt{s_{NN}} > 100$ GeV. Furthermore, the antiparticle/particle ratios measured at $\sqrt{s_{NN}} = 2.76$ TeV are consistent with 1 at all centralities; hence, we have set all chemical potentials to zero and the free parameters of the fit are 2 or 3: temperature, normalization, and, optionally, γ_S .

As a first step, we have fitted the measured multiplicities to the basic version of the SHM with $\gamma_S = 1$ (see Table IV). For the most central collisions, we confirm previous findings [22], as well as recent analysis by different groups [38] with a $\chi^2/\text{dof} \simeq 17/8$ and an overestimation of proton yields by

TABLE IV. Results of the fits to the SHM for different centralities at $\sqrt{s_{NN}} = 2.76$ TeV. First and second columns, results of the traditional fit to SHM with γ_S and with γ_S fixed to 1; third and fourth columns, same, but with afterburning corrections to the theoretical yields.

Centrality		Plain SHM fit	Plain SHM fit $\gamma_S = 1$	SHM + afterburning	SHM + afterburning $\gamma_S = 1$
0%–5%	T (MeV)	154.5 ± 3.8	157.2 ± 4.1	164.1 ± 3.4	167.3 ± 3.8
	γ_S	1.082 ± 0.059	1	1.071 ± 0.043	1
	χ^2/dof	14.23/7	18.52/8	7.66/7	10.95/8
5%–10%	T (MeV)	155.1 ± 3.9	158.8 ± 5.1	164.1 ± 3.5	168.0 ± 4.4
	γ_S	1.116 ± 0.058	1	1.086 ± 0.042	1
	χ^2/dof	17.99/7	29.54/8	9.76/7	16.31/8
10%–20%	T (MeV)	157.2 ± 4.7	162.3 ± 5.6	164.7 ± 4.6	170.0 ± 5.2
	γ_S	1.128 ± 0.066	1	1.099 ± 0.055	1
	χ^2/dof	20.86/7	34.27/8	15.73/7	23.97/8
20%–30%	T (MeV)	157.7 ± 4.8	162.9 ± 6.3	165.8 ± 4.4	171.3 ± 5.6
	γ_S	1.141 ± 0.071	1	1.111 ± 0.053	1
	χ^2/dof	22.95/7	38.02/8	13.23/7	22.52/8
30%–40%	T (MeV)	160.2 ± 5.0	162.8 ± 6.0	167.3 ± 4.9	170.5 ± 5.9
	γ_S	1.113 ± 0.073	1	1.099 ± 0.060	1
	χ^2/dof	24.40/7	33.84/8	17.52/7	24.95/8
40%–50%	T (MeV)	160.0 ± 4.8	163.0 ± 5.3	166.8 ± 4.9	169.8 ± 5.1
	γ_S	1.088 ± 0.065	1	1.068 ± 0.057	1
	χ^2/dof	20.71/7	26.72/8	16.21/7	19.85/8
50%–60%	T (MeV)	157.8 ± 4.0	157.8 ± 4.0	164.1 ± 3.7	163.8 ± 3.6
	γ_S	0.999 ± 0.058	1	0.980 ± 0.045	1
	χ^2	12.85/7	12.85/8	8.21/7	8.44/8
60%–70%	T (MeV)	153.6 ± 3.6	153.3 ± 5.2	159.0 ± 4.0	157.8 ± 5.2
	γ_S	0.843 ± 0.051	1	0.843 ± 0.050	1
	χ^2/dof	5.59/7	14.36/8	3.13/7	12.39/8

about 2σ along with an underestimation of pion yield by 1.4σ (see Table V), which seems to be a common feature of SHM fits to high energies [8]. For the midperipheral bins, the fit quality is significantly worse, with a $\chi^2/\text{dof} \simeq 31/7$ and larger discrepancies for both pions and protons, as well as for Ξ . It has been shown that in peripheral bins [25–27] the corona of single NN collisions makes strange particle yields lower than expected from a source at full chemical equilibrium. Therefore,

we introduce γ_S as a free parameter to take the effect of corona into account. This, as expected, improves the fit quality (see Table IV) considerably in the most peripheral bin, where the corona effect is more important. In other bins, it improves the fit, although not enough to make it statistically significant.

It should be noted that the chemical freeze-out temperature, in both versions, with and without γ_S , is larger in the midperipheral bin than in central (see Fig. 4) collisions. To

TABLE V. Comparison between measured [13,29] and fitted midrapidity densities of particle species in most central Pb + Pb collisions at $\sqrt{s_{NN}} = 2.76$ TeV. In the plain SHM fits, either with or without γ_S , there is an overestimation of proton and an underestimation of pion yields. The modification factors predicted by URQMD improve the agreement between data and the model for those particles. Also shown is predicted midrapidity density of deuterons assuming they are formed at hadronization according to SHM and (for the afterburning case) that they are later suppressed with the square of the modification factor calculated for protons.

Particle	Measurement	Plain SHM fit $\gamma_S = 1$	Plain SHM	SHM + afterburning $\gamma_S = 1$	SHM + afterburning
π^+	733 ± 54	659.2	645.7	694.2	683.2
π^-	732 ± 52	659.2	645.7	694.2	683.2
K^+	109.0 ± 9.0	116.0	121.2	112.1	116.8
K^-	109.0 ± 9.0	116.0	121.2	112.1	116.8
p	34.0 ± 3.0	39.69	36.64	38.62	35.93
\bar{p}	33.0 ± 3.0	39.69	36.64	38.62	35.93
Λ	26.1 ± 2.8	21.90	21.55	22.77	22.39
Ξ^-	3.57 ± 0.27	3.246	3.427	3.239	3.384
Ξ^+	3.47 ± 0.26	3.246	3.427	3.239	3.384
$\Omega + \bar{\Omega}$	1.26 ± 0.22	1.112	1.237	1.327	1.444
D			0.115		0.118

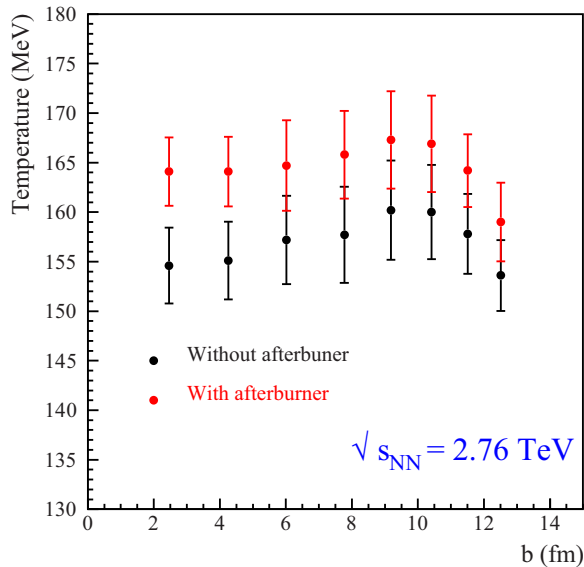


FIG. 4. (Color online) Temperature as a function of the impact parameter b (central values corresponding to centralities measured by ALICE). Black dots, chemical freeze-out temperature; red dots, LCEP (see text) temperature obtained by including URQMD modification factors.

assess the significance of the difference, one should take into account that the errors on fit parameters are strongly correlated, as is apparent from Fig. 4 because so are the errors on particle multiplicities measured in the different centrality bins. The increase of temperature toward peripheral bins is observed for the first time and it is in qualitative agreement with the idea of an afterburning stage, which, if present, has to depend on the total multiplicity as discussed in Sec. II. Thus, the more central the collision, the longer the time spent in the colliding hadronic stage and the larger the shift from hadronization temperature (assumed to be constant) down to the chemical freeze-out. This effect was studied in a previous paper of ours [17] at energies available at SPS.

The results of the fit including corrections for afterburning are shown in the third column of Table IV. The theoretical yields are calculated by multiplying the output from SHM (after strong and electromagnetic decays) by the modification factors defined in the previous section. Therefore, the fitted thermodynamical parameters (essentially temperature) supposedly pertain to the source at its latest state of chemical equilibrium, i.e., LCEP, before hadronic collisions set in. In a more refined calculation, one would use the thus-determined LCEP conditions to compute modification factors with isothermal Cooper-Frye transition at that temperature and refit the LCEP temperature until the procedures converge. Nevertheless, already in the present calculation the fitted temperature at hydro-URQMD transition (158.2 MeV, see Sec. III) is close to the final fitted value of 164 MeV, showing that we are not far from full self-consistency. The improved calculations are already in progress [39].

As can be seen from Fig. 5, the fit quality improves throughout after the implementation of afterburning corrections. The fitted temperature rises by several MeV, as shown in Fig. 4,

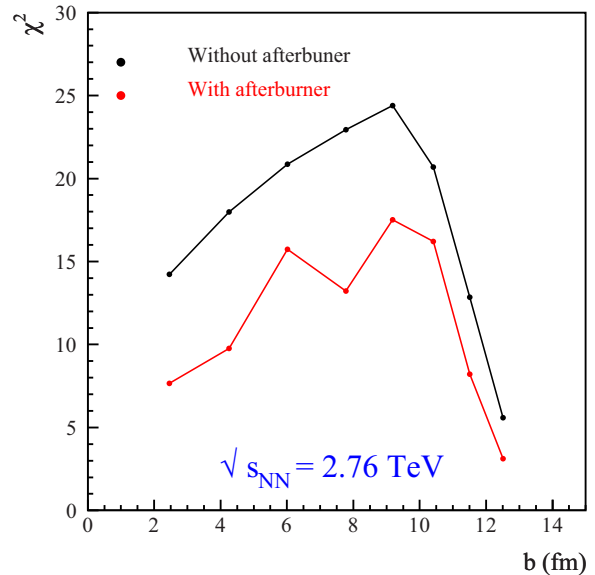


FIG. 5. (Color online) χ^2 of the SHM fits with and without afterburning corrections as a function of the impact parameter b (central values corresponding to centralities measured by ALICE). The fitted parameters being in this case T , γ_s , and the normalization; the number of degrees of freedom is 7.

in agreement with our previous findings [22]. Furthermore, the LCEP temperature is less centrality dependent than the plain chemical freeze-out temperature, which bears out the idea of a universal (at fixed baryon density) hadronization temperature [9,10]. This is best seen in Fig. 6, where we show the difference between the corrected temperature and

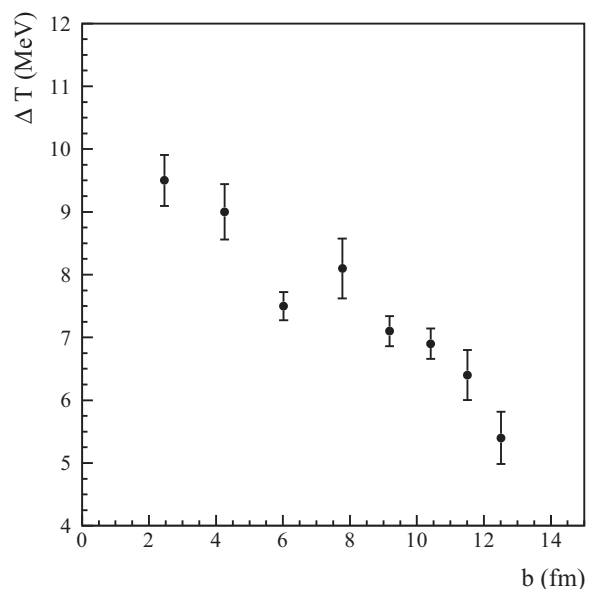


FIG. 6. Difference between the corrected temperature and the chemical freeze-out temperature as a function of the impact parameter b (central values corresponding to centralities measured by ALICE). The error bar has been estimated by taking a 100% correlation between the errors on T in the two fits.

the plain SHM fitted one. The difference steadily decreases towards peripheral collisions, again in full agreement with the picture that afterburning affects less the chemical composition if the overall multiplicity is lower. There remain two small structures in the temperature vs centrality plot after the afterburning correction: a mild rise towards midperipheral collisions (see Fig. 4) and a sizable decrease in most peripheral collisions. The former could be a residual of similar behavior seen in the plain fits that the presently calculated correction factors were not able to completely remove. Hopefully, a new calculation of correction factors with isothermal hydro-URQMD transition [39] could be able to work it out. The latter could be, however, a spurious corona effect of superposition of NN collisions with hadrons from the plasma which we are not presently able to understand in detail. Both effects will be the subject of further investigation.

V. CONCLUSIONS

To summarize, we have demonstrated that in the high-multiplicity environment of relativistic heavy ion collisions at $\sqrt{s_{NN}} = 2.76$ TeV the inelastic collisions play a significant role in modifying the primordial hadronic yields from hadronization. The amount of inelastic rescattering is expected to depend on multiplicity and, hence, on centrality. This effect is clearly seen in the centrality dependence of specific particle ratios measured by the ALICE experiment and especially Ξ/π , which—for the first time—is observed to increase towards

peripheral collisions before dropping. In the framework of the SHM, this phenomenon implies a slight dependence of the chemical freeze-out temperature as a function of centrality, which is actually observed. Once suitable correction factors, estimated through the transport model URQMD, are introduced, primordial particle multiplicities turn out to be in better agreement with a chemically equilibrated source at a nearly constant temperature of about 164 MeV. The difference between the chemical freeze-out temperature and the reconstructed latest chemical equilibrium temperature, arguably coinciding with the hadronization temperature, decreases smoothly from central to peripheral collisions, as expected in this picture. Further calculations of modification factors are in preparation to investigate the remaining small structures seen in the behavior of temperature as a function of centrality. These findings are in excellent agreement with the concept of a universal statistical hadronization occurring at the pseudocritical QCD temperature.

ACKNOWLEDGMENTS

Part of the work of F.B. was carried out over a sabbatical at the University of Frankfurt and FIAS, Frankfurt. We acknowledge the support of the Deutsche Forschungsgemeinschaft (DFG), the Hessian LOEWE initiative through HIC for FAIR, and the Istituto Nazionale di Fisica Nucleare (INFN). Computational resources were provided by the LOEWE Frankfurt Center for Scientific Computing (LOEWE-CSC).

-
- [1] T. Bhattacharya, M. I. Buchoff, N. H. Christ, H.-T. Ding, R. Gupta, C. Jung, F. Karsch, Z. Lin *et al.*, *Phys. Rev. Lett.* **113**, 082001 (2014), and references therein.
- [2] G. Endrodi, Z. Fodor, S. D. Katz, and K. K. Szabo, *J. High Energy Phys.* 04 (2011) 001; S. Borsanyi, G. Endrodi, Z. Fodor, S. D. Katz, S. Krieg, C. Ratti, and K. K. Szabo, *ibid.* 08 (2012) 053.
- [3] P. Cea, L. Cosmai, M. D’Elia, A. Papa, and F. Sanfilippo, *Phys. Rev. D* **85**, 094512 (2012).
- [4] R. Stock, *Phys. Lett. B* **456**, 277 (1999).
- [5] F. Karsch, *Central Eur. J. Phys.* **10**, 1234 (2012); A. Bazavov *et al.*, *Phys. Rev. Lett.* **109**, 192302 (2012); S. Mukherjee and M. Wagner, *PoS CPOD* **2013**, 039 (2013).
- [6] P. Alba, W. Alberico, R. Bellwied, M. Bluhm, V. Mantovani Sarti, M. Nahrgang, and C. Ratti, *Phys. Lett. B* **738**, 305 (2014); S. Borsanyi, Z. Fodor, S. D. Katz, S. Krieg, C. Ratti, and K. K. Szabo, *Phys. Rev. Lett.* **113**, 052301 (2014).
- [7] F. Becattini, *J. Phys. G* **23**, 1933 (1997), and references therein.
- [8] J. Cleymans and H. Satz, *Z. Phys. C* **57**, 135 (1993); P. Braun-Munzinger, J. Stachel, J. P. Wessels, and N. Xu, *Phys. Lett. B* **365**, 1 (1996); F. Becattini, M. Gazdzicki, and J. Sollfrank, *Eur. Phys. J. C* **5**, 143 (1998); P. Braun-Munzinger, D. Magestro, K. Redlich, and J. Stachel, *Phys. Lett. B* **518**, 41 (2001); A. Baran, W. Broniowski, and W. Florkowski, *Acta Phys. Polon. B* **35**, 779 (2004); W. Florkowski, W. Broniowski, and M. Michalec, *Acta Phys. Pol.*, **B 33**, 761 (2002); J. Cleymans, B. Kampfer, M. Kaneta, S. Wheaton, and N. Xu, *Phys. Rev. C* **71**, 054901 (2005); F. Becattini, M. Gazdzicki, A. Keranen, J. Manninen, and R. Stock, *ibid.* **69**, 024905 (2004).
- [9] H. Satz, *Int. J. Mod. Phys. E* **21**, 1230006 (2012) and references therein.
- [10] F. Becattini, [arXiv:0901.3643](https://arxiv.org/abs/0901.3643) [hep-ph] and references therein.
- [11] S. A. Bass and A. Dumitru, *Phys. Rev. C* **61**, 064909 (2000).
- [12] L. Milano (ALICE Collaboration), *Nucl. Phys. A* **904-905**, 531c (2013).
- [13] B. Abelev *et al.* (ALICE Collaboration), *Phys. Rev. C* **88**, 044910 (2013).
- [14] A. Andronic, P. Braun-Munzinger, and J. Stachel, *J. Phys. G* **35**, 054001 (2008); A. Andronic, P. Braun-Munzinger, K. Redlich, and J. Stachel, *Nucl. Phys. A* **904**, 535c (2013).
- [15] T. Anticic *et al.* (NA49 Collaboration), *Phys. Rev. C* **83**, 014901 (2011).
- [16] F. Becattini, J. Manninen, and M. Gazdzicki, *Phys. Rev. C* **73**, 044905 (2006).
- [17] F. Becattini, M. Bleicher, T. Kollegger, M. Mitrovski, T. Schuster, and R. Stock, *Phys. Rev. C* **85**, 044921 (2012).
- [18] J. Steinheimer, J. Aichelin, and M. Bleicher, *Phys. Rev. Lett.* **110**, 042501 (2013).
- [19] R. Stock, F. Becattini, M. Bleicher, T. Kollegger, T. Schuster, and J. Steinheimer, *PoS CPOD* **2013**, 011 (2013).
- [20] Y. Pan and S. Pratt, [arXiv:1210.1577](https://arxiv.org/abs/1210.1577) [nucl-th].

- [21] M. Petran, J. Letessier, V. Petracek, and J. Rafelski, *Phys. Rev. C* **88**, 034907 (2013).
- [22] F. Becattini, M. Bleicher, T. Kollegger, T. Schuster, J. Steinheimer, and R. Stock, *Phys. Rev. Lett.* **111**, 082302 (2013).
- [23] S. A. Bass *et al.*, *Prog. Part. Nucl. Phys.* **41**, 255 (1998); M. Bleicher *et al.*, *J. Phys.* **G25**, 1859 (1999); H. Petersen, J. Steinheimer, G. Burau, M. Bleicher, and H. Stöcker, *Phys. Rev. C* **78**, 044901 (2008); H. Petersen, M. Bleicher, S. A. Bass, and H. Stöcker, [arXiv:0805.0567](https://arxiv.org/abs/0805.0567) [hep-ph].
- [24] U. Heinz and G. Kestin, *PoS CPOD* **2006**, 038 (2006).
- [25] J. Adams *et al.* (STAR Collaboration), *Phys. Rev. Lett.* **92**, 112301 (2004).
- [26] J. Adams *et al.* (STAR Collaboration), *Phys. Rev. Lett.* **98**, 062301 (2007).
- [27] J. Manninen and F. Becattini, *Phys. Rev. C* **78**, 054901 (2008).
- [28] S. Das (STAR Collaboration), *Nucl. Phys. A* **904–905**, 891c (2013).
- [29] B. B. Abelev *et al.* (ALICE Collaboration), *Phys. Lett. B* **728**, 216 (2014); *Phys. Rev. Lett.* **111**, 222301 (2013).
- [30] T. Anticic *et al.* (NA49 Collaboration), *Phys. Rev. C* **86**, 054903 (2012); NA49 data compilation, <https://edms.cern.ch/file/1075059/4/na49compil20130801.pdf>.
- [31] T. Anticic *et al.* (NA49 Collaboration), *Eur. Phys. J. C* **65**, 9 (2010); C. Alt *et al.* (NA49 Collaboration), *ibid.* **45**, 343 (2006); NA49 data compilation, <https://edms.cern.ch/file/1075059/4/na49compil20130801.pdf>.
- [32] B. I. Abelev *et al.* (STAR Collaboration), *Phys. Rev. C* **79**, 034909 (2009).
- [33] B. I. Abelev *et al.* (STAR Collaboration), *Phys. Rev. C* **75**, 064901 (2007).
- [34] B. Abelev *et al.* (ALICE Collaboration), *Phys. Lett. B* **717**, 162 (2012); **712**, 309 (2012).
- [35] F. Becattini and J. Manninen, *J. Phys. G* **35**, 104013 (2008); *Phys. Lett. B* **673**, 19 (2009).
- [36] J. Steinheimer, S. Schramm, and H. Stöcker, *Phys. Rev. C* **84**, 045208 (2011).
- [37] R. Rapp and E. V. Shuryak, *Phys. Rev. Lett.* **86**, 2980 (2001).
- [38] J. Stachel, A. Andronic, P. Braun-Munzinger, and K. Redlich, *J. Phys. Conf. Ser.* **509**, 012019 (2014).
- [39] F. Becattini, M. Bleicher, E. Grossi, J. Steinheimer, and R. Stock (unpublished).